

**NASA Technical Memorandum 107697**

1N-05  
130531  
P.16

**MULTIPLE-FUNCTION MULTI-INPUT/  
MULTI-OUTPUT DIGITAL CONTROL AND  
ON-LINE ANALYSIS**

**Sherwood T. Hoadley, Carol D. Wieseman, and  
Sandra M. McGraw**

**October 1992**

(NASA-TM-107697) MULTIPLE-FUNCTION  
MULTI-INPUT/MULTI-OUTPUT DIGITAL  
CONTROL AND ON-LINE ANALYSIS  
(NASA) 16 p

N93-13565

Unclass



National Aeronautics and  
Space Administration

**Langley Research Center**  
Hampton, Virginia 23665-5225

G3/05 0130531



# MULTIPLE-FUNCTION MULTI-INPUT/MULTI-OUTPUT DIGITAL CONTROL AND ON-LINE ANALYSIS

Sherwood T. Hoadley\*, Carol D. Wieseman\*\*  
NASA Langley Research Center, Hampton, VA 23681-0001

and

Sandra M. McGraw\*\*\*  
Lockheed Engineering and Sciences Co., Hampton, VA 23666

## ABSTRACT

The design and capabilities of two digital controller systems for aeroelastic wind-tunnel models are described. The first allowed control of flutter while performing roll maneuvers with wing load control as well as coordinating the acquisition, storage, and transfer of data for on-line analysis. This system, which employs several digital signal multi-processor (DSP) boards programmed in high-level software languages, is housed in a SUN Workstation environment. A second DCS provides a measure of wind-tunnel safety by functioning as a trip system during testing in the case of high model dynamic response or in case the first DCS fails. The second DCS uses National Instruments LabVIEW Software and Hardware within a MacIntosh environment.

## INTRODUCTION

Wing flutter is an aeroelastic phenomenon occurring at certain flight conditions in which the natural vibrations of the wing are amplified by aerodynamic forces. If not properly accounted for in the design of the aircraft, flutter can occur and cause catastrophic breakage of a wing. Passive means for preventing flutter include changing the stiffness, mass or planform of the wing or limiting the flight envelope by avoiding the flight conditions at which it occurs. These passive means invariably reduce aircraft performance.

A major thrust of modern research has been to actively control unfavorable aeroelastic phenomena using aerodynamic control surfaces on the wing. These phenomena include flutter, resulting from aerodynamic forces acting on the aircraft, maneuver loads, resulting from rolling maneuvers, and gust loads, resulting from flying through turbulence. For active control, control-law equations are executed by a digital computer to determine control surface commands based upon signals from sensors located on the aircraft which describe either the vehicle motion or loads. This computerized system is referred to as a digital controller system (DCS). Current types of digital control/analysis requirements involved in sophisticated wind-tunnel and flight testing require

sophisticated solutions. The primary objective of this paper is to present the current types of digital control/analysis requirements involved in sophisticated wind-tunnel testing. Figure 1 depicts several actively controlled wind-tunnel models which have been or will be tested at the NASA Langley Research Center using the digital controller systems described herein.

In the mid-1980s, Rockwell International Corporation (ref.1) pioneered and advanced a concept referred to as an Active Flexible Wing (AFW). This concept exploited wing flexibility to provide weight savings and improved aerodynamic performance. The use of active controls for flutter suppression, gust load alleviation, and maneuver load alleviation also provides a capability for reducing vehicle weight. By taking full advantage of active controls and the AFW concept, Rockwell predicted that weight savings of at least 15 percent of take-off gross weight could be achieved for an advanced fighter configuration. The aeroelastically-scaled wind-tunnel model shown in figure 1(a) provided a testbed for the AFW program (ref.2). Current research involves an actively controlled wind-tunnel model in the Benchmark Models Program designed for Benchmark Active Controls Testing (BACT). This model, shown in figure 1(b), will primarily allow the acquisition and study of aerodynamic data at the onset of flutter and provide a testbed for studying the use of spoilers as well as a trailing edge control surface as active control devices. Future models, depicted in figure 1(c), will employ, among others, the use of piezoelectric actuators as active control devices.

This paper is organized in the following manner. First, an overview, including both hardware and software components, of the active digital controller system (ADCS) used in the previously mentioned wind-tunnel tests (refs. 3 and 4) is presented. Next, the real-time processing requirements for the ADCS, including the generic forms of control-law implementation, are described. Descriptions of the on-line data acquisition and real-time analysis capabilities of the ADCS are also presented. Following this is an overview, including both hardware and software components, of the passive digital controller system (PDCS) and on-line frequency analyzer used in the aforementioned BACT program. The presentation will conclude with comments about the limitations of both systems with an emphasis on future needs.

## ACTIVE DIGITAL CONTROLLER SYSTEM (ADCS)

One of the primary purposes of the Active Flexible Wing 1991 wind-tunnel test and the basic ADCS requirements

\* Senior Aerospace Engineer, Aeroservoelasticity Branch, MS 243, NASA Langley Research Center, Hampton, VA, 23681-0001

\*\* Aerospace Engineer, Aeroservoelasticity Branch, MS 243, NASA Langley Research Center, Hampton, VA, 23681-0001

\*\*\* Electrical Engineer, Lockheed Engineering and Sciences Company, MS 243, NASA Langley Research Center, Hampton, VA 23681-0001

was to perform various types of roll control testing both below and above the open-loop flutter boundary using a digital controller system. The open-loop flutter boundary is defined to be the boundary beyond which the vehicle would flutter if no flutter suppression system was actively employed in the loop (closed-loop). Figure 2 outlines those basic requirements. The ADCS allowed simultaneous control of flutter while performing one of three rolling maneuvers, the last two with wing load control. These four control systems, depicted in the figure, were a Flutter Suppression System (FSS), a Roll Trim System (RTS), a Rolling Maneuver Load Alleviation System (RMLA), and a Roll Rate Tracking System (RRTS). The FSS could be switched on or off, independent of which roll control system was operating. To provide active digital control, analog sensor signals from the model were first passed through necessary antialiasing and notch filters and then converted to digital signals within the digital controller. The ADCS then processed these signals through a digital flutter suppression system and/or one of three types of digital roll control systems. After the various control-law outputs were calculated, they were combined and converted to analog signals to be sent to the model as actuator commands.

#### Basic Design Constraints

The basic design of the ADCS was constrained by various requirements which limited, as indicated in figure 3, the way in which the system could be designed. For example, besides the multiple function requirements discussed in the preceding subsection, each type of control law was to be implemented in different ways, using different combinations of sensors and actuators. Another requirement was the ability to modify control-law equations, even during the test, so no finalized control laws could be implemented. Furthermore, most of the hardware had already been selected prior to designing the system. A final requirement was that the real-time system had to operate at guaranteed fixed cycling rates which were much faster than even the fastest cycling frequency of the HOST time-share operating system, namely 60Hz. These various constraints determined the basic design.

#### Overview of the Hardware Components

The ADCS operates within, but independently of, a slower host operating system within a SUN Workstation environment. It synchronizes the operation of four different processing units, allowing flexibility in form and functionality of control-law equations. For the AFW tests, it operated at a regulated speed of 200Hz. It also coordinated the acquisition, storage, and transfer of data for on-line analysis.

Figure 4 presents an overview of the hardware components in the system. The ADCS is housed in a SUN workstation. The items on the left depict the basic time-share system. The SUN's HOST CPU performs all the user/interface and time-share functions, including those involving disk storage, tape, and network communications. Depicted on the right are those dedicated boards which comprise the real-time system, each performing individual functions. The first board, labeled C1, is a SKY Computers, Inc. Challenger 1 integer DSP, with two TMS 32020 microprocessors, which functions as the real-time executor, controlling all real-time activities. The second board, labeled C30, is a SKY Computers, Inc. Challenger C30/V

multiprocessor board, which functions as the primary control-law processor. This floating-point dual processing board contains two TMS 320C30 processing nodes. These nodes share common global memory, while operating simultaneously. The third board, labeled AP, is a SKY Computers, Inc. Warrior I floating point array processor. This board functions as the backup control-law processor if the C30 fails; however, in the real-time environment, it is not capable of executing the multiple control laws at the rates required of the ADCS for flutter suppression, so the C30 with two processing nodes was used as the primary control-law processor for multiple function control. The last four boards depicted on the right side of the SUN Workstation are analog-to-digital (AID) and digital-to-analog (DIA) conversion boards. The AID boards digitize up to sixty-four (64) incoming analog signals, and the DIA boards convert sixteen (16) outgoing digital commands to analog signals.

The interface electronics, depicted on the right-hand-side of figure 4, are housed in a rack which includes a Filter Box, a Patch Box, and a Status Display Panel. Antialiasing and notch filter cards for up to 64 incoming channels are contained in the Filter Box for processing signals from the model. The Patch Box simply provides a means to connect signals to the model or from the simulator directly to the cables coming from the ADCS. The Status Display Panel displays the real-time status of the ADCS such as the current mode of operation and whether the control loop to the model is open or closed.

#### Overview of the Software Components

Figure 5 presents an overview of the software components in the ADCS. As mentioned previously, the user interface functions are performed on the HOST CPU. These include a user/controller interface program which sends the matrices (or tables) defining the various control laws to the control-law processor and backup processor prior to testing. This user/controller interface program also provides interactive instructions to the real-time executor during testing. This includes such items as instructions to open or close a control loop. The information display program displays information from the real-time system such as actuator commands, error messages, etc. and it transfers temporarily stored blocks of sampled data from direct access storage to the disk so that new data can be saved without destroying previously sampled data. The data transfer program processes the sampled data and transfers subblocks across the network for on-line data analysis.

The real-time system, which operates at fixed rates, (200Hz for the AFW and BACT testing) is comprised of the real-time executor (C1), the control-law processor (C30), the array processor (AP), data translation boards, and direct access memory. The real-time executor controls all the real-time tasking. This includes acquiring digitized sensor signals from the AID boards, sending sampled sensor inputs to the C30 (or AP), starting control-law processing on either the C30 (or AP), and outputting the actuator commands to the DIA boards to be converted to discretized analog signals. It also stores sampled data for on-line analysis in direct access storage. During AFW wind-tunnel testing, the C30 executed a selected roll control law on one of its processing nodes and the FSS control law on the other. The AP backup processor provided backup control-law execution for either the FSS or the RMLA

system, but not both. For BACT wind-tunnel testing, some of the control-law functions are different, but they, too, are processed on the C30.

### Basic Modes of Operation

There were seven basic modes of operation for the AFW wind-tunnel tests. The first three did not involve the execution of a control law. These modes are also required for the BACT wind-tunnel tests. The first is a MAINTENANCE mode. In this mode, all the signals passing through the analog/digital conversion boards can be checked out. The second is a MANUAL mode. This mode allows individual positioning of the control surfaces and check-out of the scaling and calibration of all incoming and outgoing signals. The third is a STATIC mode. This mode is designed primarily to acquire experimental data about the open-loop model or plant without any control laws operating.

The other modes of operation include the operation of at least one control law. They are named according to which control-law processing was considered dominant. Data acquired in each mode relates directly to the primary control law evaluation. For the AFW tests, they were FSS, RTS, RMLA, and RRTS, corresponding to the four control-law systems tested. The generic formulations of the control-law equations for each of these modes will be presented in subsequent sections.

The ADCS as used for the AFW tests has been modified for use in the BACT wind-tunnel testing. There are three primary differences. First, there are no roll-control modes of operation for that model. Second, the control surfaces and sensors are different. Third, there are other types of control functions which employ a variation of the generic formulations of control equations that were used in the ADCS for the AFW. This variation will be presented in a subsequent section.

### Generic State-space Formulation of Control Equations

Figure 6 depicts the implementation of control laws using a generic state-space formulation in which there is only a one time-step delay between the incoming and outgoing signals. The matrices defining these control equations are provided by the control-law designers and downloaded prior to testing. In this type of formulation, the sensor signals can first be blended in some fashion to form the control-law inputs, and outputs can be distributed among various control surfaces. These blending and distribution matrices were also provided by the control-law designer. In this implementation, the control-law outputs are converted to left and right actuator commands by the real-time executor, combined with other actuator commands and sent out to the model by the real-time executor.

### Bilinear Table Look-up

The generic form of one of the roll control functions for the AFW tests was a bilinear, table look-up procedure as depicted in figure 7. Six tables of actuator commands, which were functions of the roll-rate and roll-rate error, were provided by the control-law designer. The actual command output values were bilinearly interpolated from these tables. Above the open-loop flutter boundary, these were added to the FSS control-law outputs before being sent to the model.

### Rolling Maneuver Command

The command used during rolling maneuvers of the AFW was computed by the real-time executor of the ADCS. The basic format of the rolling maneuver command is shown in figure 8. The model would first be rolled to a specified initial roll angle and held there by the RTS until the roll-rate command was initiated. Then the executor would ramp the command up to a peak specified value,  $p_L$ , at a specified rate,  $\dot{p}_{Lon}$ , and then hold that command until it determined that the model had passed a specified termination angle,  $\Phi_T$ . As soon as the termination angle was passed, the command was ramped back down toward zero at a rate of  $\dot{p}_{Loff}$ . After the roll-rate slowed sufficiently, reaching a predetermined "capture" rate,  $p_{cap}$ , the RTS would again take over control of the model, holding the model at the current roll angle until a new roll-angle command was specified. The rolling maneuver load control laws actually operated only while the roll maneuver was being executed. The RTS operated before and after each maneuver.

### Multi-Rate Formulation of Multi-function Control Equations

Figure 9 depicts the current implementation of multi-rate control laws to be implemented during testing of the BACT model. This implementation uses generic state-space formulations in which each set of equations can perform different functions, such as flutter control and gust load alleviation, operating simultaneously, but at different rates. The control-law processor executes a state-space formulation of each control law provided by the control-law designers. A requirement of this system is that information calculated in one system be cross fed to the other as desired by the control-law designer.

### Timing Requirements

The timing requirements for each real-time execution cycle in the ADCS, during AFW wind-tunnel testing, which involved the processing of a control law are shown in figure 10. The times shown here are for an execution time of 5ms, the time required for the sampling frequency of 200Hz. Referring to the figure, times are approximate for all control law execution modes. It took approximately 0.15ms to acquire all the control-law (CL) outputs from the control-law processor generated in the preceding cycle, and 0.8ms to combine them and send them to the digital-to-analog converters. Approximately 1.7ms were used to process the incoming signals, about 0.5ms to send the signals to the control-law processor and start execution, and 0.7ms to store sampled data in direct access storage. There were various functions, such as sending out discrete signals or reading operator instructions, which did not need to be performed at 200Hz. These were grouped into ten groups and performed at a slower rate (one-tenth of the 200Hz rate). At most 0.2ms were used for each of these "slow-cycle" functions. At the end of 5.0ms, the next cycle would start. Execution of the control laws had to be performed during the time the control-law processor was started and the end of the cycle. To insure completion, the C30 set a flag to indicate execution was finished. The C1 would wait, if necessary, for this flag before acquiring the CL outputs and starting the next cycle.

For all the wind-tunnel tests performed with the AFW using the ADCS as described herein, all executions, including those executed by the C30, were completed within one time cycle.

## GENERAL ON-LINE ANALYSIS REQUIREMENTS

Wind-tunnel testing and the use of active digital controllers imposes some essential requirements for on-line system analysis both before, during, and after wind-tunnel testing. Figure 11 presents an overview of these requirements. One requirement is to perform control law verification by verifying the correct operation of each control law as implemented by the ADCS both before and during testing. Controller performance evaluation is also essential. Closed-loop testing can be dangerous, especially above the flutter boundary. Analysis tools are required that predict whether a control law will destabilize the system, before closing the loop; i.e., before allowing command signals calculated by the controller to be sent to the model. Analysis tools are also required, after closing the loop, which indicate that minimum margins of stability are maintained as testing proceeds beyond the open-loop flutter boundary. Determination of the plant (or model) dynamics (or equations of motion) from experimental data can be used to improve control laws (as well as improve the plant equations of motion for simulation). Another important analysis capability in this type of testing is the ability to predict the actual open-loop flutter boundary while running closed-loop. Details of the controller performance evaluation and on-line analysis capabilities are provided in refs. 5-7.

Following a discussion of hardware required for on-line analysis, the primary categories of analyses: ADCS validation, controller performance evaluation, plant determination, and open- and closed-loop stability boundary prediction will be discussed.

### On-line Analysis Hardware

Figure 12 shows the hardware used for the on-line analysis during AFW and BACT wind-tunnel testing. The hardware consists of two SUN 3/160 work stations configured with some similar processing boards, one of which is the fast array processor described earlier. The first SUN workstation (SUN-1) is used for the ADCS. During ADCS operation, selected data can be saved in binary form and transferred as a binary data file to the second sun workstation (SUN-2) via an Ethernet line. This process is fairly fast (approximately 5 seconds) for the amount of data analyzed on-line and solves networking and data compatibility problems. The on-line analysis calculations are performed on the SUN-2. The array processor (with 25 MFLOPS operating speed) is capable of computing all the transfer functions within a time frame which allows for near real-time processing, taking only a couple of minutes to provide any of the plots for Controller Performance Evaluation described below.

### ADCS Validation

Sample control-law transfer function comparisons, for one FSS control law used during the AFW tests, are shown in figure 13. In order to verify proper control law execution, these transfer functions were generated using on-line analysis

tools. Transfer function plots of this form indicate the ratio of the magnitude of an output signal to an input signal over a specified frequency range of excitation. The phase plot indicates the number of degrees the output signal lags (or leads) the input signal at each frequency. Every time a new control law is loaded into the ADCS, plots of this type are generated which compare the ADCS control-law transfer function with analytically generated data provided by the control-law designer. Discrepancies between the two curves must be accounted for before testing can proceed.

In order to validate the operation of the ADCS, frequency domain transfer functions or time-domain response verifications were performed at many stages of ADCS development and testing. The various stages of comparison are indicated below:

- Open-loop (controller only)
- Open-loop with antialiasing and other signal conditioning filters included
- Closed-loop during Real-time simulation, prior to wind-tunnel testing
- Closed-loop during wind-tunnel testing

### Controller Performance Evaluation - Time Domain

Time domain plots of the type shown in figure 14 were used to evaluate controller performance during the AFW tests during commanded maneuvers of the AFW wind-tunnel model. The upper plot shows the roll rate and the lower shows the roll angle. The dashed line in the upper plot is the commanded roll rate; the solid white line is the measured roll rate, and the curve in the bottom figure is the roll angle. Control-law designers used these to evaluate how well their control law caused the model to follow the commanded rolling maneuver. By comparing plots of loads during rolling maneuvers, reductions or control of loads could be verified. This method was used to evaluate control laws which attempted to reduce or control loads by comparing results with a similar control law which did not. Data for fourteen different signals were saved and could be plotted to gain insight into system behavior during a rolling maneuver. References 8 and 9 show the use of these time-domain analyses in presenting overall controller performance for the various rolling maneuver control systems which were tested on the AFW model.

### Controller Performance Evaluation - Frequency Domain

Flutter suppression wind-tunnel testing requires various controller performance analysis capabilities. The capability to predict the closed-loop stability margins prior to closing the loop is required. By identifying potentially destabilizing control laws and consequently not closing the loop with these control laws, the model and the wind-tunnel are protected from damage. Furthermore, if the closed-loop system would only be marginally stable, the loop is not closed. After closing the loop, the stability margins of the system still need to be determined. Minimum stability margins are normally required as testing proceeds beyond the open-loop flutter boundary. Furthermore, when the control laws are multi-input multi-output, single transfer function analysis is not sufficient for evaluating the performance of the control laws and establishing stability margins; hence, more sophisticated analyses requiring complex matrix manipulations

must be performed. Frequency domain plots of the type shown in figure 15 are used to evaluate controller performance. Each of these represents various ways of measuring closed-loop robustness and open-loop plant stability.

In particular, this figure shows the output generated for a closed-loop flutter suppression system above the open-loop flutter boundary. The upper two plots show the minimum and maximum singular values of the return difference matrices. The minimum singular value is related to combined gain and phase margins of a multi-input/multi-output control system and gives a measure of closed-loop system stability margin. Specifically, these two plots provide measures of robustness with respect to multiplicative uncertainty at the plant input and plant output points, respectively. The lower left plot provides a measure of robustness to additive uncertainty. In all three, horizontal lines were drawn at 0.1, 0.2, and 0.3 of the singular values in order to quickly identify a marginally stable system. The determinant plot at the lower right provides a means of checking open-loop stability. Although, it is not clear in this figure that the determinant plot encircles the origin, enlarging the plot to better identify encirclements does reveal one. An encirclement of the origin in this case identifies that the model was above the open-loop flutter boundary. References 5 and 6 provide detailed information on the types of analyses required for this type of controller performance evaluation.

The capability of generating Nichols plots (not shown here) in order to view determinant data in a manner which not only shows encirclements but also provides gain and phase margin information is also available. References 10 - 13 show the use of these analyses in presenting overall controller performance for the various flutter suppression systems tested on the AFW model.

### Plant Determination

As stated previously, determination of actual plant dynamics from experimental data can be used to improve control laws. Open-loop plant determination was used to improve control-law design for one of the control laws tested during the AFW wind-tunnel tests. The open-loop plant transfer functions developed from experimental data were supplied to the control-law designers, and new control laws developed using this data were then tested (ref. 11).

The entire open-loop transfer matrix can be obtained regardless of which control law is being tested. The matrix calculations required are those indicated in the table shown in figure 16. The "c" subscript refers to control-law elements, The "e" refers to elements of the system external to the control law. A by-product of the frequency domain CPE discussed earlier is the calculation of the subsection of open-loop plant transfer matrix, labeled  $G_{cc}$  in figure 16. The remainder of the plant is obtained by exciting the additional control surfaces not used by the control law, measuring additional sensors not used by the control law, and then performing the indicated matrix operations for  $G_{ec}$ ,  $G_{ce}$ , and  $G_{ee}$ . Details of this plant determination are provided in references 7. These same types of operations may be used in the future to provide on-line learning to adaptive controllers.

### Open-loop Flutter Prediction

Flutter boundary prediction uses results obtained from the open-loop plant determination (ref. 7). The procedure and

an example of determining the open-loop flutter boundaries is shown in figure 17. Once the plant has been determined, the inverse maximum singular value (IMSV) is calculated and plotted as a function of frequency. A sample plot at one test point is shown at the left. The minimum of this curve is then determined. The minimum IMSV and the frequency at which the minimum occurs are then plotted as a functions of the dynamic pressures of the various test points. These are shown in the plot at the right. The point at which the minimum IMSV goes to zero is the predicted open-loop flutter point. The dynamic pressure at which this occurs is the open-loop flutter dynamic pressure,  $q_f$ . The frequency at that point corresponds to the open-loop flutter frequency,  $f_f$ . At the end of the wind-tunnel tests, a flutter point was determined from open-loop testing in which no FSS control laws were operating. Applying the technique described herein, the predicted open-loop flutter boundary for the AFW wind-tunnel model using closed-loop results compared well with later open-loop experimental results. These results are shown in the table at the bottom of figure 17.

### Closed-loop Flutter Prediction

During closed-loop testing, it is desirable to predict the closed-loop flutter boundary. This is the point at which the closed-loop system (with FSS operating) will go unstable. One mechanism to determine this is to perform peak-hold analysis. This is a process in which the peak value at each frequency of the auto spectra of a signal is calculated and plotted over time using overlapped processing. The dynamic pressure at which the reciprocal of this peak-hold data approaches 0 indicates the closed-loop flutter boundary and the frequency at which it would occur is the predicted closed-loop flutter frequency. These results, which are not shown, also compared well with other sources. Details of this analysis technique are provided in ref. 7.

## PASSIVE DIGITAL CONTROLLER SYSTEM (PDCS)

The PDCS has been developed to provide a measure of safety during wind-tunnel testing. The PDCS uses National Instruments LabVIEW Software and Hardware within a Macintosh environment, but does not actively employ sensor signals from the wing to compute control surface commands. The LabVIEW icon-based programming environment provides a fundamentally convenient mechanism for programming digital controllers.

The PDCS provides a measure of safety in testing of models in the wind tunnel by monitoring signals and by functioning as a trip system. If specified limits of certain signals such as accelerations, wing deflections, or control surface rates, are exceeded, the PDCS 'trips' the wind-tunnel causing bypass valves to be opened and dynamic pressure to drop. It also takes command of the control surfaces from the ADCS and commands the control surfaces to predetermined positions. In many cases, this will save a model from damage once flutter has occurred. Figure 18 indicates the connectivity between the ADCS, the PDCS, and other hardware components.

Additional requirements of the PDCS are static deflection of control surfaces to specified positions and

excitation of the control surfaces either singly or in combination. Figure 19 is a copy (except for color enhancements) of the front panel of the PDCS, indicating the functionality of the system.

#### **PDCS Analysis Requirements**

In addition to the basic PDCS requirements, the need to develop the capability to perform frequency analysis of signals was also identified. The PDCS/Frequency Analyzer currently includes the capability to calculate dual channel frequency responses (transfer functions in the frequency domain), power spectra, power spectral densities and auto- and cross correlations of pairs of signals. It also displays blocks of each of the signals in the time-domain as each block is analyzed. Figure 20 is a sample copy (except for color enhancements) of the front panel of the PDCS/Frequency Analyzer, indicating the functionality and capabilities of the system.

#### **Overview of Hardware/Software Components**

Figure 21 presents an overview of the hardware components in the PDCS, and figure 22 indicates the basic software functionality of each hardware component. It is housed in a Macintosh II workstation. The items on the left depict the basic time-share system. The Macintosh's HOST CPU performs all the user/interface and time-share functions, including those involving disk storage and network communications. Depicted on the right are those dedicated boards which comprise the real-time system, each performing individual functions, and connected to each other via a Real-Time System Interface (RTSI) bus. Data conversions are performed by two National Instruments Corp. NB-MIO-16L multifunction I/O (MIO) boards which perform A/D and D/A input and output functions for the PDCS. Data acquired by these MIO boards is transferred to and from memory by a National Instruments NB-DMA-8-G multipurpose interface board. This board functions as a direct memory access controller (DMAC) for real-time data acquisition to increase the system throughput and free the Macintosh processor for the user/interface tasks and other applications. It provides the timing for acquiring data and for sending waveform excitations at fixed rates. In fact, the Macintosh II can be processing other applications while the DMAC performs data acquisition in the background.

### **FUTURE DCS REQUIREMENTS**

Digital controller systems in the future will need to address more complex systems than described herein and will require more parallel computing power. Some areas of future research in the use of active control of aeroelastic phenomena are presented in more detail in this section.

Flutter suppression, maneuver load alleviation, gust load alleviation, and other active control functions are progressing toward adaptive control. In the future, control laws will adapt on-line to 1) system changes, such as failure of sensors or loss of actuators and other control devices, and 2) model changes, such as the loss of some mass or changes in stiffness or damping. References 14 and 15 indicate this trend. This adaptability might include on-line learning of the actual plant dynamics and the best selection of control equations

designed with respect to certain pre-selected failure modes. This will require the use of multiple processors, running concurrently, to provide real-time plant determination and control-law modifications.

Furthermore, the more complex the system, the more important the on-line analysis capabilities, and the more complex. To provide these analysis capabilities, faster data transfer speeds and computations will be required.

#### **Neural-net Controllers**

Another avenue of research is in the use of neural-net controllers to represent the control equations as well as to characterize the plant. One motivating factor for this is the ability for neural nets to incorporate nonlinearities into control equations and simulation equations of the model. Another factor is that it provides a possible mechanism for including on-line learning and adaptability. The impetus in this area of research is indicated by references 16 and 17. Software and/or hardware tools which facilitate the implementation of neural-net controllers and neural-net equations of motion of the model will be used in the near future. Figure 23 depicts the use of neural-net control equations implemented into the ADCS structure. A neural net may replace the generic state-space and/or table look-up formulation of the control equations. Neural nets may also be used to adapt a set of control laws to changes in the model.

#### **Increasing Number of Actuators**

Active control of aeroelastic phenomena will use an ever-increasing number of actuators including flaps, ailerons, spoilers, and piezoelectric materials. In fact, the use of piezoelectrics as actuators to induce strain to suppress flutter or reduce wing loads is coming into the forefront of research. In the near future, the use of piezoelectric actuators will result in an order of magnitude increase in actuators, with possibly a corresponding number of actuator command signals. The need to monitor the failure of each of these actuators in addition to monitoring other types of sensors used in active control of aeroelastic phenomena will require the ability to monitor over 100 sensor signals. A/D conversion of these increasing number of sensors as well as D/A conversion of the increasing number of actuator commands will be required. In addition, many of these signals will require various forms of signal conditioning such as antialiasing and notch filtering. The hardware requirements for a basic ADCS could increase tenfold in the near future.

#### **Real-Time Simulation**

Another avenue of research is in the development of cost-effective real-time simulators for these more complex plants. Work is progressing currently to employ the second SUN Workstation, described earlier, to provide real-time simulation. It will be configured with the same dedicated processors and I/O boards as the first SUN Workstation featured in figure 4. An IRIS workstation will be connected through a fiber optic network to provide additional computing power and real-time graphics display. The use of neural nets to include nonlinearities in the plant dynamics is being explored. These areas of future research are summarized in figure 24.



### Current DCS Limitations and Possible Solutions

- Interfaces between processing units require specialized software which is dependent upon real-time executor and operating systems. Standardization or compatibility is a driving need.
- Data transfer between processors increases the delay time for on-line analysis; however, delays can be decreased with fiber-optic networks and reflective (or replicated) memory.
- Complex software must be tailored to individual needs. Programming languages which facilitate this tailoring will be used in the future, especially those which are compatible with existing systems. Icon-based programming environments can provide a fundamentally easy mechanism for programming and tailoring both digital controllers and analyzers.
- Signal conditioning is a driving need in all digital/analog systems. Flexible, low-cost programmable filtering for a large number of signals is desirable.

### CONCLUDING REMARKS

Digital Controller Systems have been developed and tested which support multiple-function control, synchronized operation of a number of computing units, fixed-rate real-time operation, and provide data acquisition for on-line analysis. Future digital controllers can be constructed similarly to these prototypes.

Near real-time data reduction and analysis capabilities are a vital part of a test effort. They provide control-law designers and test managers with important information which guide the testing sequence and allow optimum use of wind-tunnel test time. Before a test, control-law verification must be performed and used by the digital control system designer to validate the digital controller system. During the test, analyses provide a means of protecting the model and the wind tunnel from damage and provide the control-law designers with quantitative measures for analyzing their control-law performance. After the test, the same analysis capabilities can be used to provide further data reduction and analyses.

Digital controller systems in the future will need to address more complex systems than described herein and will require more parallel computing power. Hardware and software products which allow convenient, cost-effective mechanisms for implementation of this research will be utilized in the near future.

### REFERENCES

1. Perry, B. III; Cole, S.; and Miller, G: *A Summary of the Active Flexible Wing Program*, AIAA Paper No. 92-2080-CP, presented at the AIAA Dynamics Specialists Conference, Dallas, Texas, April 16-17, 1992.
2. Perry, B. III; Mukhopadhyay, V.; Hoadley, S.T.; et al: *Digital-Flutter-Suppression-System Investigations for the Active Flexible Wing Wind-Tunnel Model*, AIAA Paper No.90-1074-CP, presented at the AIAA/ASME/ASCE/AHS 31<sup>st</sup> Structures, Structural Dynamics, and Materials Conference, Long Beach, California, April 1990. Also published as NASA TM-102618, March 1990.
3. Hoadley, S.H.; Buttrill, C.S.; McGraw, S.M.; and Houck, J.A.: *Development, Simulation Validation, and Wind-Tunnel Testing of a Digital Controller System for Flutter Suppression*. Paper presented at the Fourth Workshop on Computational Control of Flexible Aerospace Systems, July 11-13, 1990, Williamsburg, Virginia. NASA CP 10065, March 1991, pp.583-613.
4. Hoadley, S.T.; McGraw, S.M.: *The Multiple-Function Multi-Input/Multi-Output Digital Controller System For The AFW Wind-Tunnel Model*, AIAA Paper No. 92-2083-CP, presented at the AIAA Dynamics Specialists Conference, Dallas, Texas, April 16-17, 1992.
5. Pototzky, A.S.; Wieseman, C.D.; Hoadley, S.T.; and Mukhopadhyay, V.: *Development and Testing of Methodology for Evaluating the Performance of Multi-Input/Multi-Output Digital Control Systems*. AIAA Paper No. 90-3501, presented at the AIAA Guidance, Navigation, and Control Conference, Portland, Oregon, August 20-22, 1990.
6. Pototzky, A.S.; Wieseman, C.D.; Hoadley, S.T.; and Mukhopadhyay, V.: *On-Line Performance Evaluation of Multi-Loop Digital Control Systems*. AIAA Journal of Guidance, Control and Dynamics, July-Aug 1992, pp. 878-884.
7. Wieseman, C.D.; Hoadley, S.T.; and McGraw, S.M.: *On-line Analysis Capabilities Developed to Support the AFW Wind-Tunnel Tests Wing Program*, AIAA Paper No. 92-2084-CP, presented at the AIAA Dynamics Specialists Meeting, Dallas, Texas, April 16-17, 1992.
8. Woods-Vedeler, J.A.; and Pototzky, A.S.: *Rolling Maneuver Load Alleviation Using Active Controls*. AIAA Paper No. 92-2099-CP, presented at the AIAA Dynamics Specialists Meeting, Dallas, Texas, April 16-17, 1992.
9. Moore, D.B.: *Maneuver Load Control Using Feedforward Commands*. AIAA Paper No. 92-2100-CP, presented at the AIAA Dynamics Specialists Meeting, Dallas, Texas, April 16-17, 1992.
10. Mukhopadhyay, V.: *Flutter Suppression Digital Control Law Design and Testing for the AFW Wind-Tunnel Model*. AIAA Paper No. 92-2095-CP, presented at the AIAA Dynamics Specialists Meeting, Dallas, Texas, April 16-17, 1992.
11. Christhilf, D.M.; and Adams, W.M.Jr.: *Multifunction Tests of a frequency Domain Based Flutter Suppression System*. AIAA Paper No. 92-2096-CP, presented at the AIAA Dynamics Specialists Meeting, Dallas, Texas, April 16-17, 1992.

12. Waszak, M.R.; and Srinathkumar, S.: *Flutter Suppression for the Active Flexible Wing: Control System Design and Experimental Validation*. AIAA Paper No. 92-2097-CP, presented at the AIAA Dynamics Specialists Meeting, Dallas, Texas, April 16-17, 1992.
13. Klepl, M.J.: *A Flutter Suppression System Using Strain Gauges Applied to Active Flexible Wing Technology*. AIAA Paper No. 92-2098-CP, presented at the AIAA Dynamics Specialists Meeting, Dallas, Texas, April 16-17, 1992.
14. Peloubet, Jr., Bolding, R. M., and Penning, K. B.: *Adaptive Flutter Suppression Wind-Tunnel Demonstration*. AFWAL-TR-87-3053, Oct. 1987
15. Ljung, L. and Gunnarsson, S.: *Adaptive tracking in System Identification - a survey*, Automatica, Vol. 26, No. 1, 1990, pp. 7-22.
16. Narendra, K.S. and Parthasarathy, K.: *Identification and Control of Dynamical Systems Using Neural Networks*, IEEE Transactions on Neural Networks, Vol. 1, No. 1, Mar. 1990, pp. 4-27.
17. Ha, C. M., Wei, Y. P., and Bessolo, J. A.: *Reconfigurable Aircraft Flight Control System Via Neural Networks*, General Dynamics Engineering Research Report, Fort Worth Division, Texas, June, 1991.

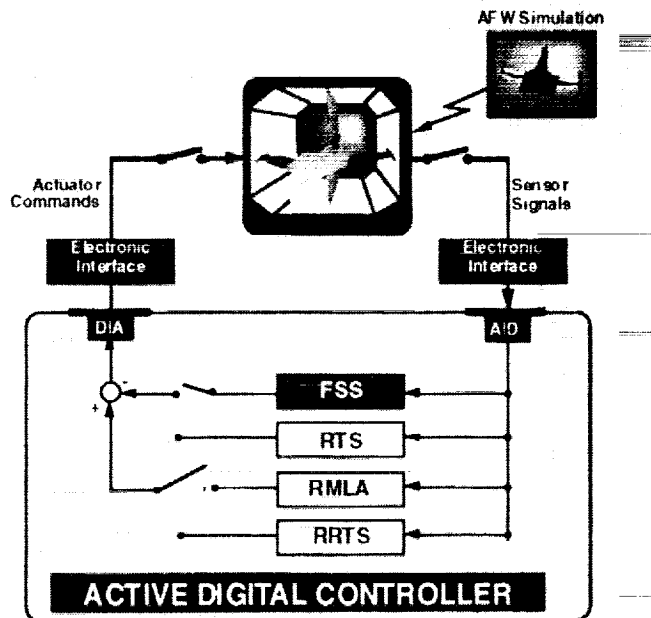


Figure 2.- ADCS performance requirements for the 1991 AFW wind-tunnel tests.

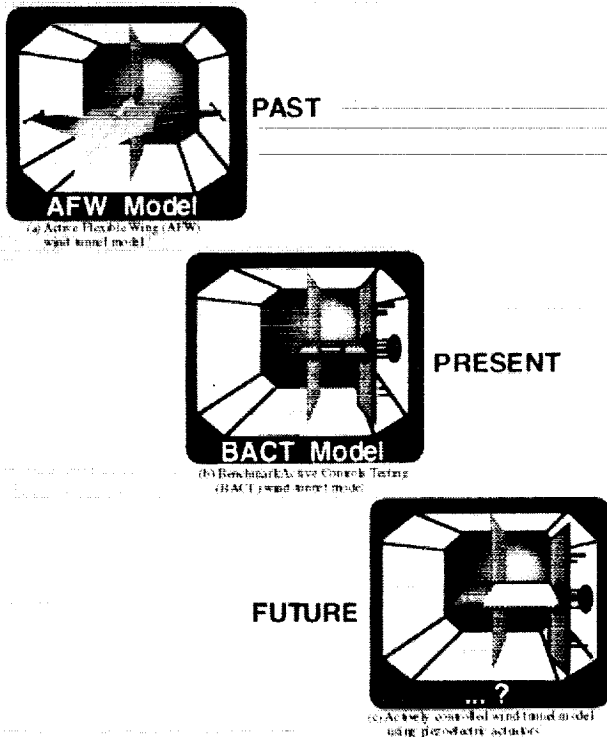


Figure 1.- Past, present, and future aeroelastic wind-tunnel models for active controls testing.

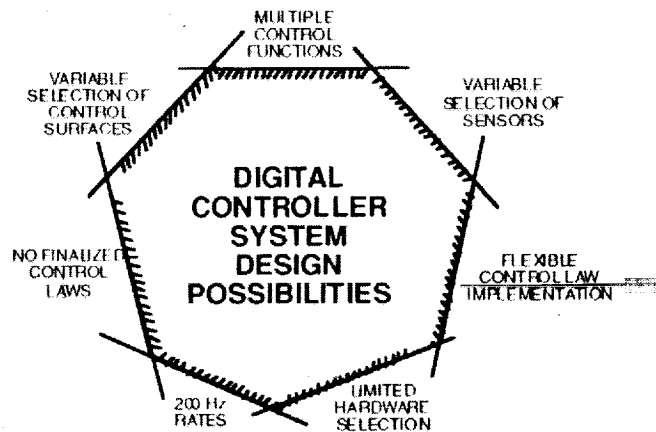


Figure 3.- Design possibilities constrained by design requirements.

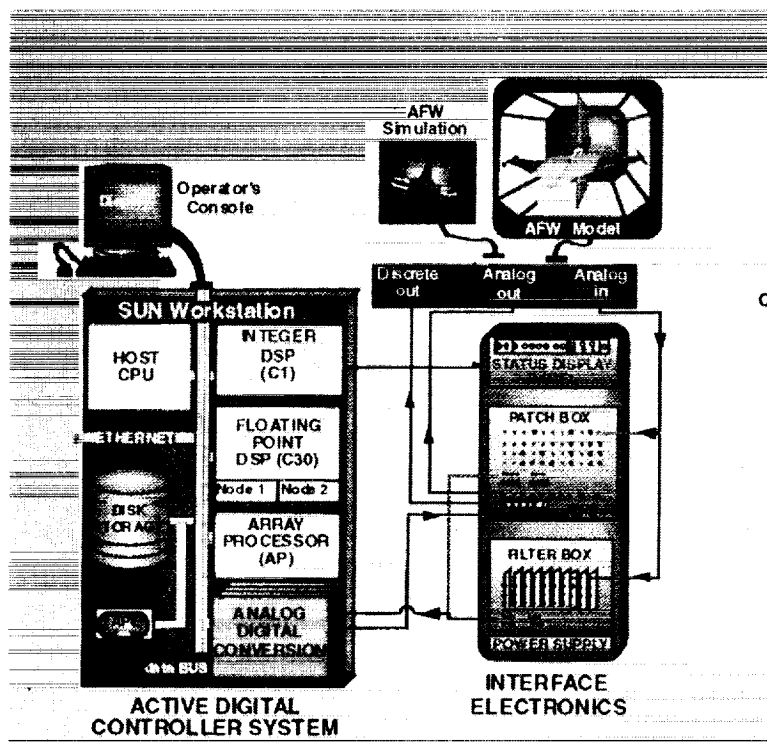


Figure 4.- Overview of hardware components in the ADCS and interface electronics to the plant.

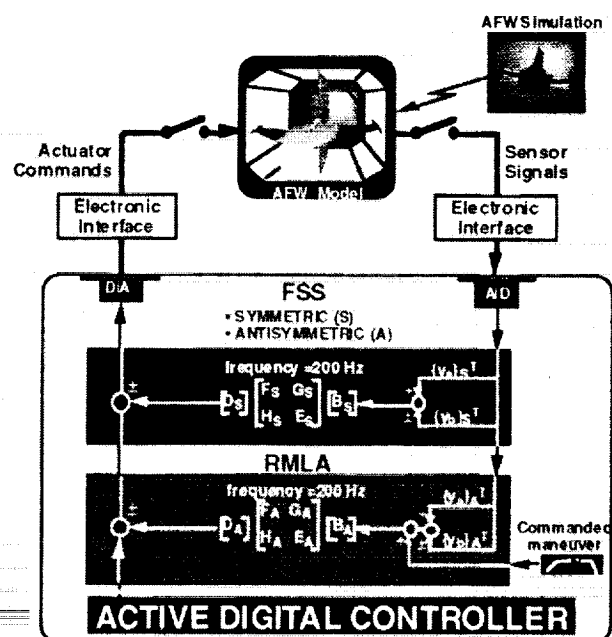


Figure 6.- Implementation of control laws using a generic state-space formulation.

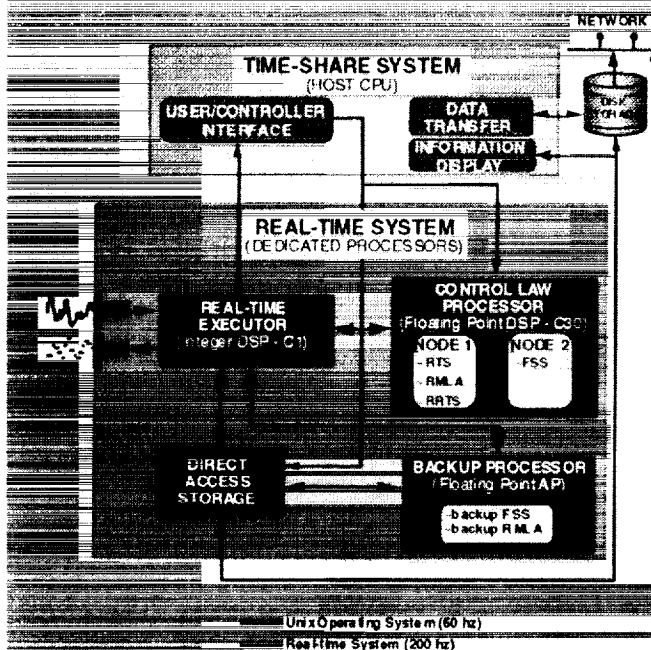


Figure 5.- Overview of software components in the ADCS.

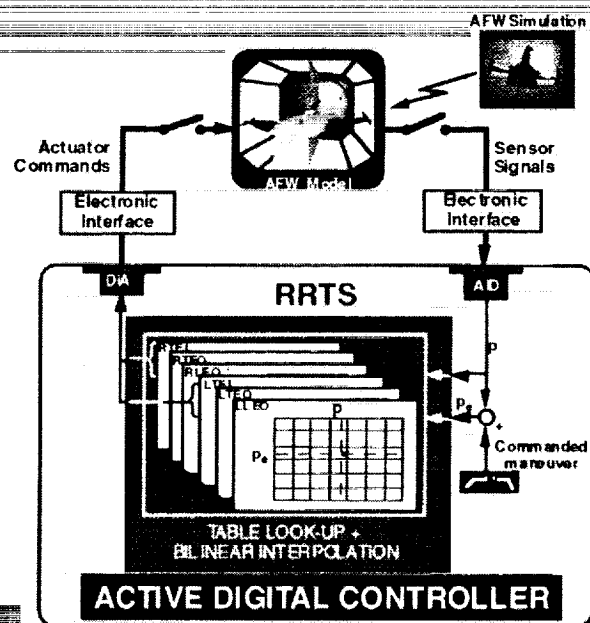


Figure 7.- Implementation of control laws using a generic table look-up formulation with bilinear interpolation.

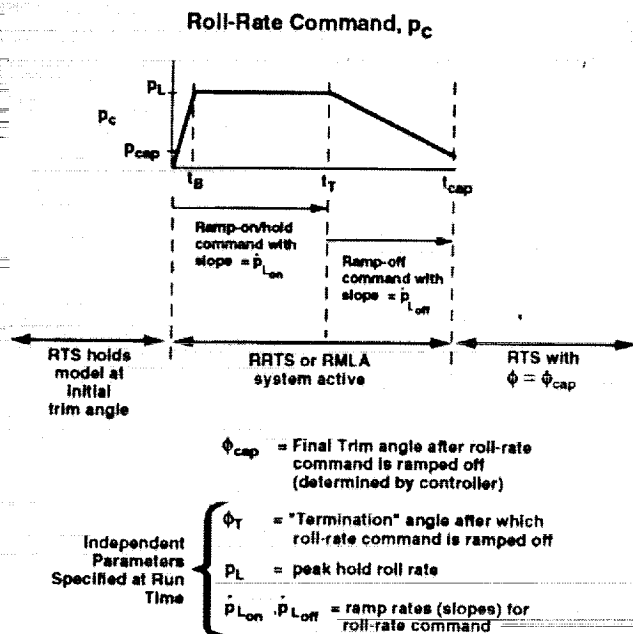


Figure 8.- Ramp-on/hold/ramp-off format of the rolling maneuver command used for the 1991 AFW wind-tunnel tests.

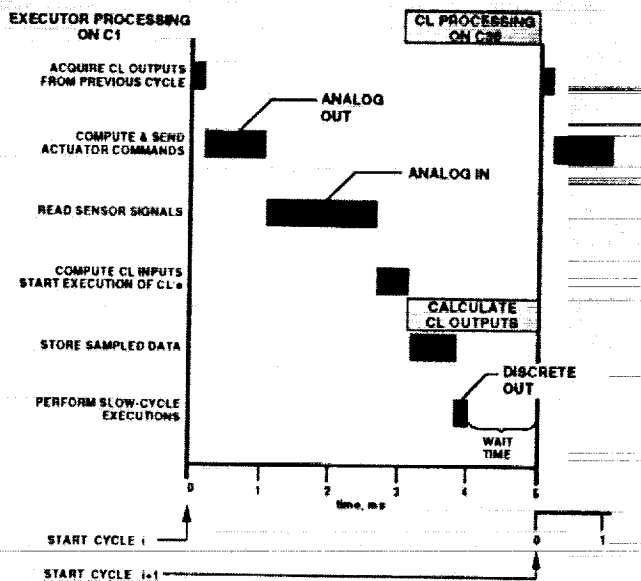


Figure 10.- Real-time execution timing requirements of ADCS for control law testing.

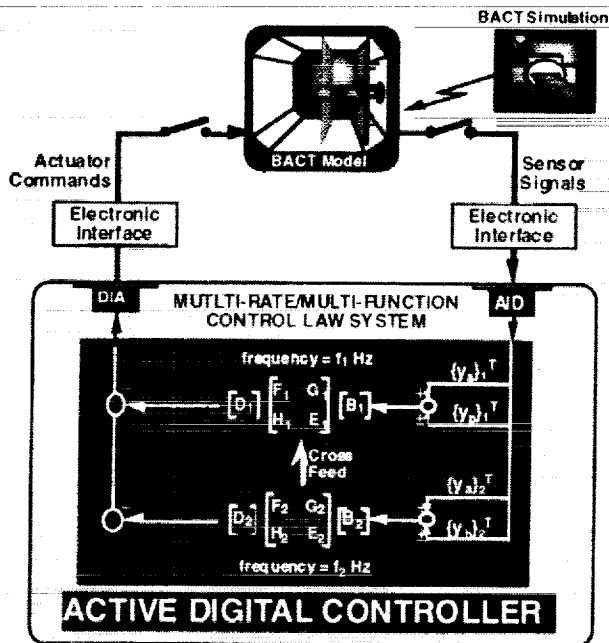


Figure 9.- Implementation of multi-rate control laws using generic state-space formulations.

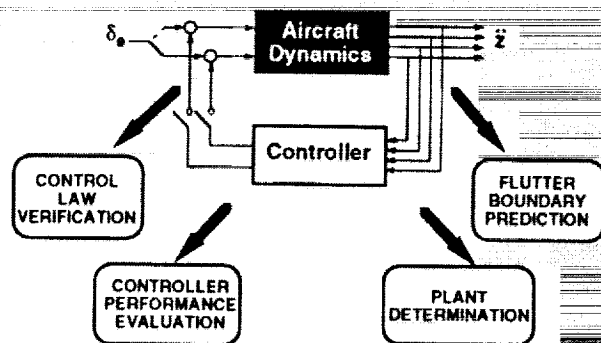


Figure 11.- Overview of on-line analysis capabilities required for AFW and BACT wind-tunnel testing.

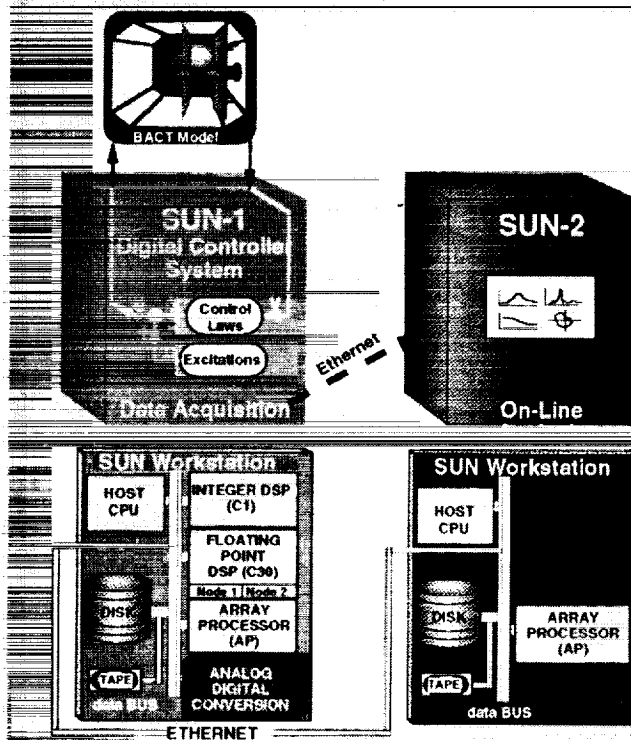


Figure 12.- On-line ADCS analysis hardware used for AFW and BACT wind-tunnel testing.

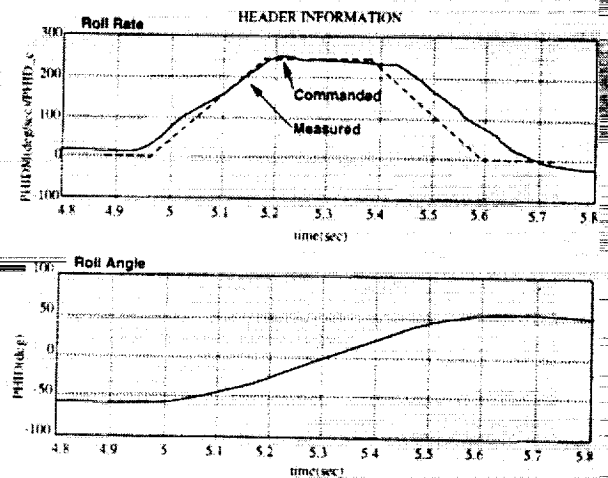


Figure 14.- Typical type analyses required for time-domain RMLA or RRTS controller performance evaluation.

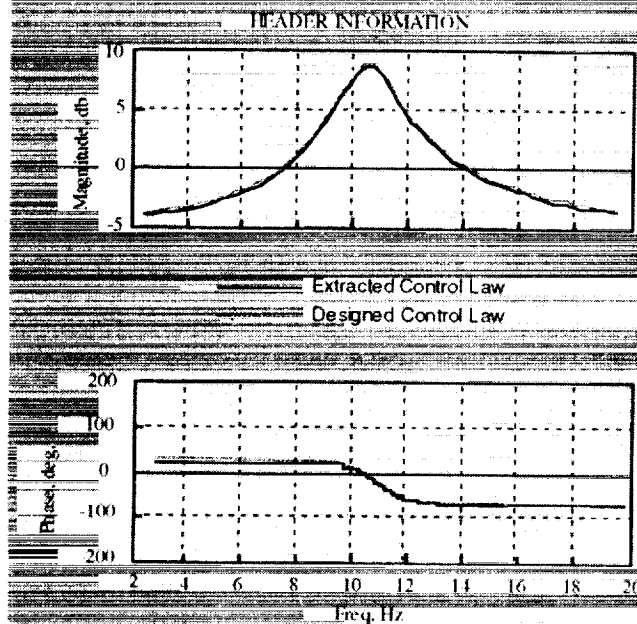


Figure 13.- Typical type analyses required for state-space control law verification and ADCS validation.

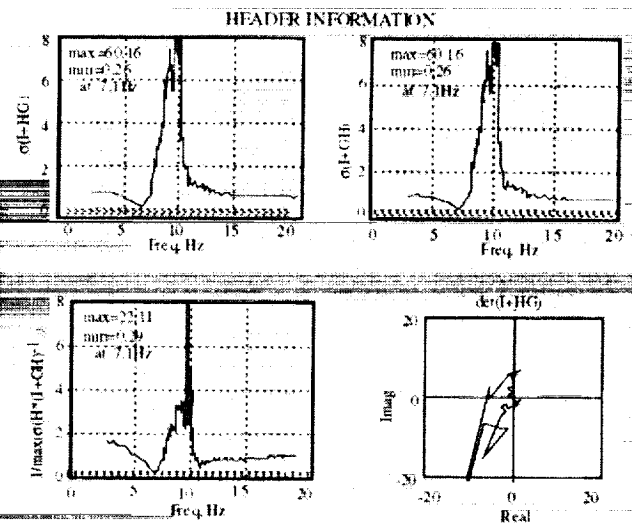


Figure 15.- Typical type analyses required for frequency-domain FSS controller performance evaluation.

## PLANT DETERMINATION

- OBTAIN ENTIRE OPEN-LOOP PLANT TRANSFER MATRIX TO
- IMPROVE PLANT MODEL (EQUATIONS OF MOTION)
  - IMPROVE CONTROL LAW DESIGN

SUBSCRIPTS  
c - refers to control law elements  
e - refers to elements external to control law

$$G = \begin{bmatrix} G_{cc} & G_{ec} \\ G_{ce} & G_{ee} \end{bmatrix}$$

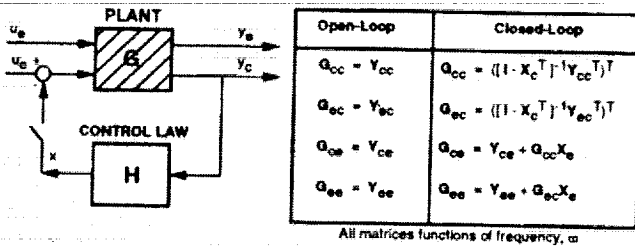


Figure 16.- Equations necessary for open-loop plant determination using data acquired during closed-loop testing.

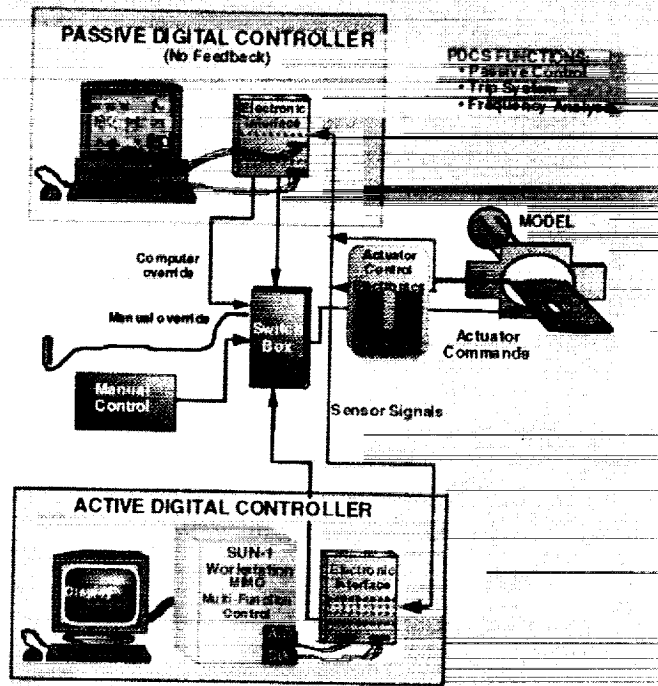


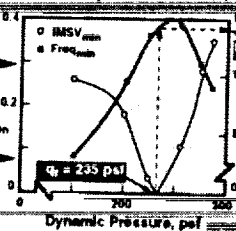
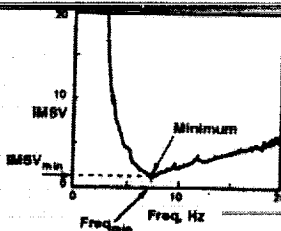
Figure 18.- Current hardware components and interfaces for digital controller systems in BACT wind-tunnel testing.

## FLUTTER BOUNDARY PREDICTION

### OPEN-LOOP FLUTTER

Compute Inverse of the Maximum Singular Value (IMSV)

Plot  $IMSV_{min}$  and  $Freq_{min}$  Versus Dynamic Pressure



FLUTTER CHARACTERISTIC RESULTS		
	Closed-Loop Prediction	Open-Loop Test Measurements
Dynamic Pressure (psf)	235	235
Frequency (Hz)	9.8	9.6

Figure 17.- Typical analyses required for open-loop flutter boundary prediction using data acquired during closed-loop testing.

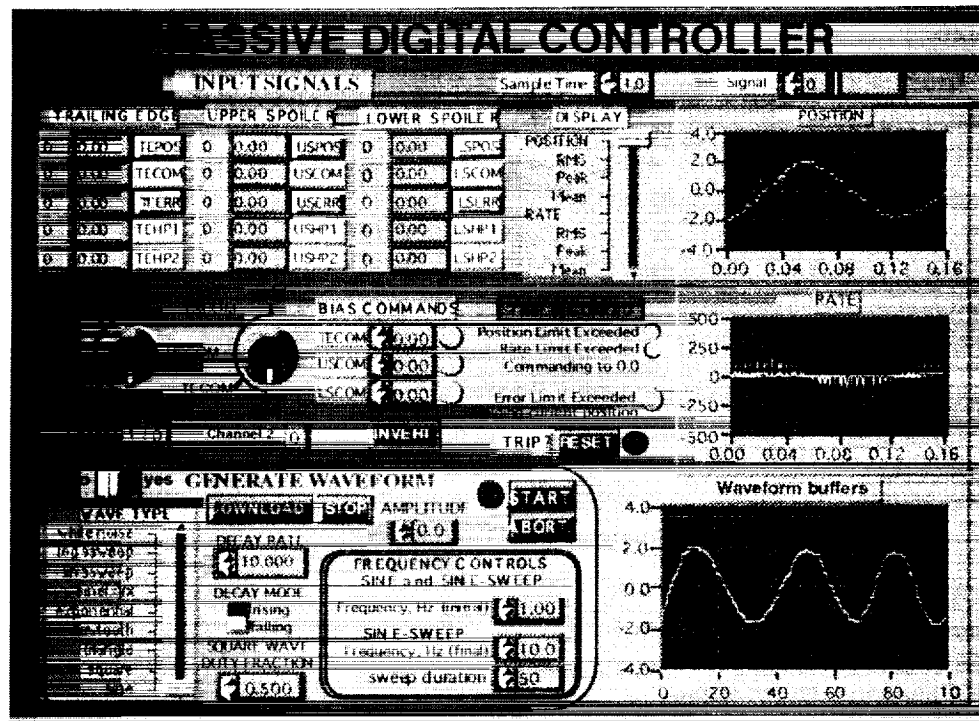


Figure 19.- PDCS front panel showing static and trip system functionality.

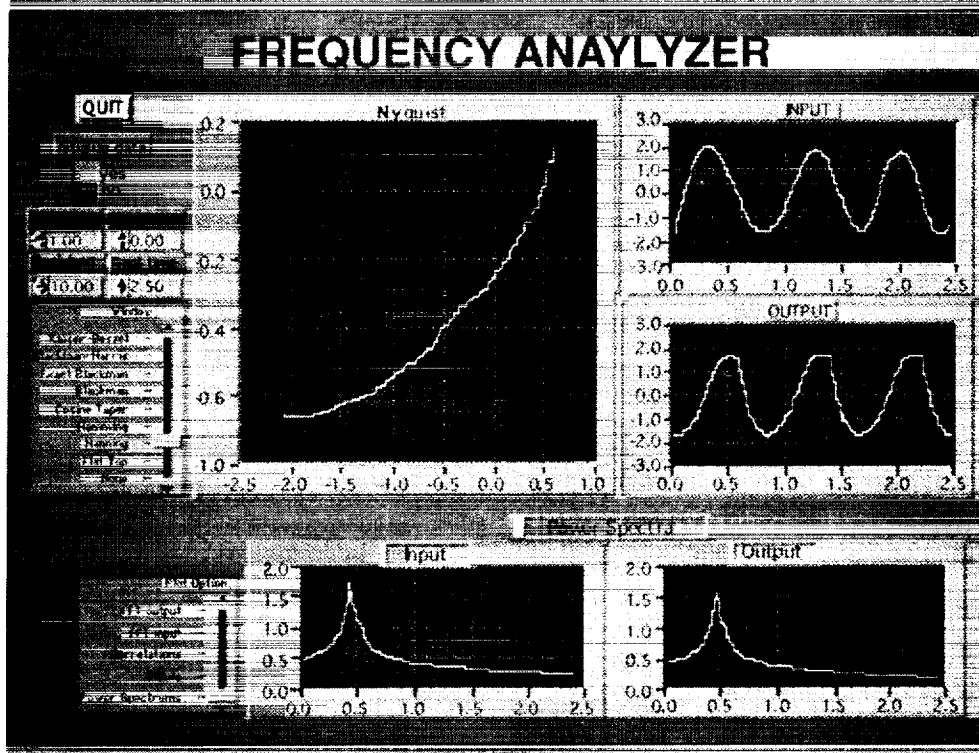


Figure 20.- PDCS Frequency analyzer front panel showing data analysis functionality.



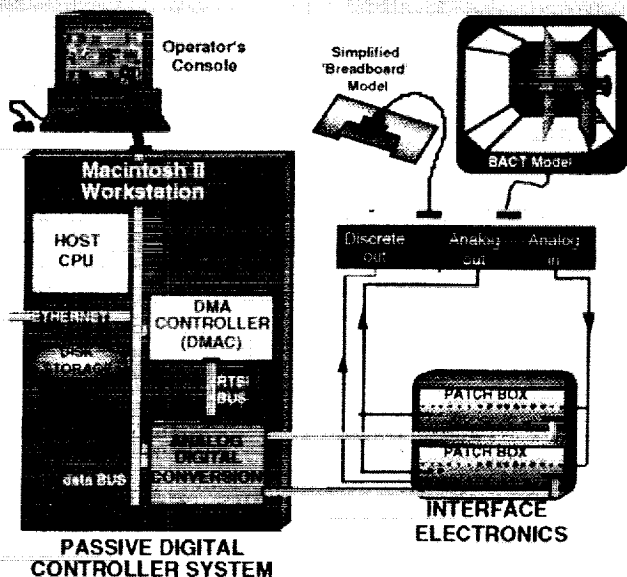


Figure 21.- Overview of hardware components in the PDCS/Frequency Analyzer and interface electronics to the plant.

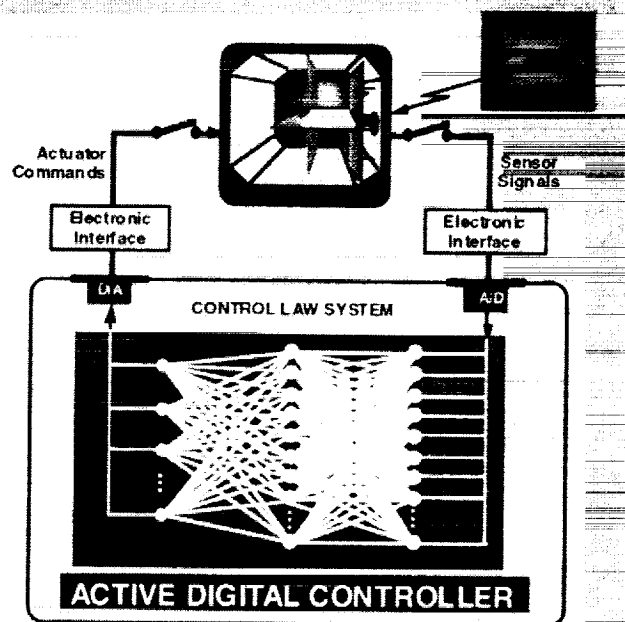


Figure 23.- Implementation of neural-net control laws by the ADCS to meet future requirements.

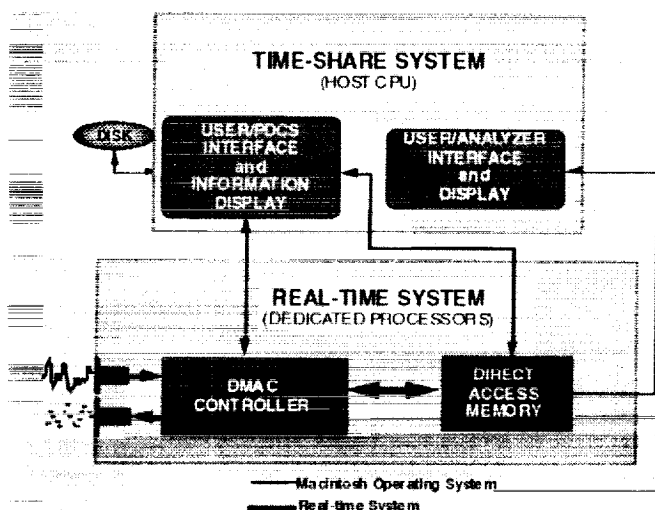
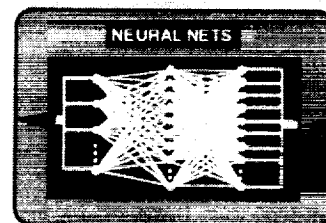


Figure 22.- Overview of software components in the PDCS/Frequency Analyzer.

## FUTURE PLANS



### DIGITAL CONTROL

- NeuralNet Formulation of Control Laws
- Adaptive Control of Changing Model
- Tolerance to Failure of Actuators/Sensors
- Use of Large Number of Actuators/Sensors

### SIMULATION

- Use SUN Workstation and Dedicated Processors for Equations of Motion
- Neural Net Modeling of Nonlinear Plant
- IRIS Workstation for Real-Time Graphics

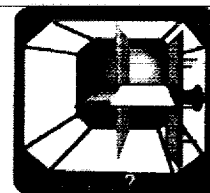


Figure 24.- Future areas of research and development for sophisticated wind-tunnel.





# REPORT DOCUMENTATION PAGE

Form Approved  
OMB No. 0704-0188

Public reporting burden for this collection of information is estimated to average 1 hour per response, including the time for reviewing instructions, searching existing data sources, gathering and maintaining the data needed, and completing and reviewing the collection of information. Send comments regarding this burden estimate or any other aspect of this collection of information, including suggestions for reducing this burden, to Washington Headquarters Services, Directorate for Information Operations and Reports, 1215 Jefferson Davis Highway, Suite 1204, Arlington, VA 22202-4302, and to the Office of Management and Budget, Paperwork Reduction Project (0704-0188), Washington, DC 20503.

1. AGENCY USE ONLY (Leave blank)		2. REPORT DATE October 1992	3. REPORT TYPE AND DATES COVERED Technical Memorandum	
4. TITLE AND SUBTITLE Multiple-Function Multi-Input/Multi-Output Digital Control and On-Line Analysis			5. FUNDING NUMBERS WU 505-63-50-15	
6. AUTHOR(S) Sherwood T. Hoadley, Carol D. Wieseman, and Sandra M. McGraw				
7. PERFORMING ORGANIZATION NAME(S) AND ADDRESS(ES) NASA Langley Research Center Hampton, VA 23681-0001			8. PERFORMING ORGANIZATION REPORT NUMBER	
9. SPONSORING/MONITORING AGENCY NAME(S) AND ADDRESS(ES) National Aeronautics and Space Administration Washington, DC 20546-0001			10. SPONSORING/MONITORING AGENCY REPORT NUMBER NASA TM-107697	
11. SUPPLEMENTARY NOTES Presented at the DSP <sup>x</sup> Exposition and Symposium, San Jose, California, October 14-16, 1992. Hoadley and Wieseman: NASA Langley Research Center, Hampton, VA; McGraw: Lockheed Engineering and Sciences Co., Hampton, VA.				
12a. DISTRIBUTION/AVAILABILITY STATEMENT Unclassified - Unlimited Subject Category 05			12b. DISTRIBUTION CODE	
13. ABSTRACT (Maximum 200 words) The design and capabilities of two digital controller systems for aeroelastic wind-tunnel models are described. The first allowed control of flutter while performing roll maneuvers with wing load control as well as coordinating the acquisition, storage, and transfer of data for on-line analysis. This system, which employs several digital signal multi-processor (DSP) boards programmed in high-level software languages, is housed in a SUN Workstation environment. A second DCS provides a measure of wind-tunnel safety by functioning as a trip system during testing in the case of high model dynamic response or in case the first DCS fails. The second DCS uses National Instruments LabVIEW Software and Hardware within a Macintosh environment.				
14. SUBJECT TERMS Active controls; aeroelasticity; aeroservoelasticity; digital controller; multifunction active controls; multi-input/multi-ouput digital control; multi-rate digital control; simulation			15. NUMBER OF PAGES 15	
			16. PRICE CODE A03	
17. SECURITY CLASSIFICATION OF REPORT Unclassified	18. SECURITY CLASSIFICATION OF THIS PAGE Unclassified	19. SECURITY CLASSIFICATION OF ABSTRACT	20. LIMITATION OF ABSTRACT	